Food Research International 62 (2014) 193–204

Contents lists available at ScienceDirect

Food Research International

journal homepage: www.elsevier.com/locate/foodres

Peptides extracted from common bean (*Phaseolus vulgaris* L.) non-digestible fraction caused differential gene expression of HCT116 and RKO human colorectal cancer cells

Diego A. Luna Vital [a,b], Guadalupe Loarca-Piña [a], Vermont P. Dia [b], Elvira González de Mejía [b,*]

[a] Programa de Posgrado en Alimentos del Centro de la República (PROPAC), Research and Graduate Studies in Food Science, School of Chemistry, Universidad Autónoma de Querétaro, Querétaro, Qro 76010, Mexico

[b] Department of Food Science and Human Nutrition, University of Illinois at Urbana–Champaign, 228 ERML, 1201 W Gregory Drive, Urbana, IL 61801, USA

ARTICLE INFO

Article history:
Received 1 December 2013
Accepted 23 February 2014
Available online 5 March 2014

Keywords:
Genes
Colorectal cancer
Beans
Peptides
Non digestible fraction

ABSTRACT

The role in cancer chemoprevention of proteins present in non-digestible fraction of common bean (*Phaseolus vulgaris* L.) is unknown. The aim was to examine the effect of peptide extracted from two cultivars of the common bean Azufrado Higuera (AH-PE) and Bayo Madero (BM-PE) on a gene expression using human colon cancer cells through a microarray analysis. HCT116 and RKO colon cancer cells were treated with 0.5 mg/mL AH-PE and BM-PE for 24 h; RNA was extracted and the gene expression was analyzed using an Agilent Low Input Quick Amp Labeling assay. In the HCT116 human cells, 511 and 964 genes were affected by the AH-PE and BM-PE treatments, respectively, with 405 genes found to be commonly affected by peptide extracts. In the RKO human cells, 45 and 32 genes were affected significantly by the AH-PE and BM-PE treatments, respectively, with 19 genes common for both extracts. Bioinformatic analysis using Database for Annotation Validation and Integrated Discovery showed that the primary genes affected were involved with oxidation–reduction, response to stimulus, protein phosphatase, MAPK signaling, selenium binding and response to wounding. Ingenuity Pathway Analysis showed that in the HCT116 cell line, NRF-2 related antioxidant enzymes were up-regulated while glutathione redox-related enzymes were down-regulated in the RKO cell line, potentially causing reactive oxygen species (ROS) imbalance. Validation of genes by RT-PCR showed good agreement for the genes with a potential role in cancer proliferation and apoptosis (PDE4B and OSGIN1, and KRT19 and EEF1A2). This study discovered, for the first time, 8 differentially expressed genes to be similar for both human colon cancer cell lines triggered by both bean cultivars, namely C11orf31, C9orf169, EMP1, GEM, PLIN2, SUN3, TRIM16L and TXNRD1.

1. Introduction

Cancer is a public health problem worldwide. It is estimated that in Latin America and the Caribbean alone, 1.1 million cancer cases will be diagnosed in 2015 and more than six thousand cancer deaths will occur annually, with colorectal cancer (CRC) representing 7% of those cases and deaths (Ferlay et al., 2013). Dietary factors such as eating habits and nutrient intake are closely related to the incidence or reduction in risk of CRC (Wolin, Carson, & Colditz, 2010). Legumes, specifically common beans which are consumed worldwide, have been associated with a decrease of colon adenoma recurrence (Lanza et al., 2006). The common bean contains significant amounts (around 44%) of non-digestible fraction (NDF) composed of soluble and insoluble fibers, resistant starch, oligosaccharides, phenolic compounds and protein and/or peptides that can be fermented and released in the colon (Vergara-Castañeda et al., 2010). It is known that NDF exerts a chemopreventive effect on colon cancer in in vivo and in vitro models through the regulation of cellular events related to apoptosis and cell cycle progression (Vergara-Castañeda, Guevara-González, Guevara-Olvera, Oomah, & Loarca-Piña, 2012; Campos-Vega et al., 2012). In vitro studies demonstrated that fermentation products of common bean NDF cultivar Bayo Madero modified the expression of human Tp53-mediated signal transduction response genes which are involved in apoptosis, cell cycle and cell proliferation (Campos-Vega et al., 2012). In addition, in the in vivo model of colon cancer azoxymethane-induced in rats fed with the total common bean NDF cultivar Bayo Madero, the regulation of genes corresponded to Tp53 pathway, being most affected GADD45A, CDKN1A, CDC25C and CCNE2 (Vergara-Castañeda et al., 2012). These effects have been attributed to the action of carbohydrate fermentation products in combination with polyphenols present in NDF; however it is worth to note the high amount of protein and/or peptides also present in NDF, for which the role in chemoprevention is unknown.

Recent attention has been given to the potential anticancer effect of peptides derived from natural sources. Peptides have high affinity and specificity for targets with low toxicity, and they also have a good tissue

* Corresponding author. Tel.: +1 217 244 3196; fax: +1 217 265 0925.
E-mail address: edemejia@illinois.edu (E.G. de Mejía).

http://dx.doi.org/10.1016/j.foodres.2014.02.037
0963-9969/

penetration due to their small size (Buthia & Maiti, 2008). Regarding the anticancer peptides in legumes, it is well known that lunasin, a 43 amino acid peptide originally found in soybean, has several chemopreventive properties, through induction of apoptosis by different mechanisms in L1210 leukemia cells (González de Mejía, Wang, & Dia, 2010), CRC cell lines HT29, RKO, KM12L4 and HCT116 (Dia & de Mejía, 2010, 2011), and in breast cancer cells in vitro and in vivo (Hsieh, Hernandez-Ledesma, & de Lumen, 2011; Hsieh, Hernandez-Ledesma, Jeong, Park, & de Lumen, 2010). These findings have shed some light on the anticancer properties of peptides present in food sources and specifically on legumes such as the common bean, which is consumed worldwide. The aim of this study was to evaluate the differentially expressed gene (DEG) profile of HCT116 and RKO human CRC cells in response to the peptide extracts of the common bean NDF cultivars Azufrado Higuera (AH-PE) and Bayo Madero (BM-PE) through the microarray analysis. Through bioinformatics tools, we found for the first time that both treatments AH-PE and BM-PE affected the genes in human colon cancer cells. For example, in HCT116 genes involved in oxidation–reduction, protein phosphatases, MAPK signaling and NRF-2 related antioxidant response were modulated. Regarding RKO some genes related to response to stimulus, selenium binding, response to wounding and glutathione redox related enzymes were differentially expressed in response to the treatments.

2. Materials and methods

2.1. Materials

The common bean (*P. vulgaris* L.) cultivars Azufrado Higuera and Bayo Madero, harvested in 2011 in Central Mexico were provided by the Instituto Nacional de Investigaciones Forestales Agrícolas y Pecuarias (INIFAP, Mexico). Human CRC cells HCT116 [positive for transforming growth factors beta 1 (TGF-β1) and beta 2 (TGF-β2) expression] (ATCC website, 2013) and RKO [lacks endogenous human thyroid hormone receptor beta 1 (h-TRbeta1)] (ATCC website, 2013), were obtained from Dr. Lee M. Ellis (MD Anderson Cancer Center, University of Texas). Eagle's Minimum Essential Medium and 0.25% (w/v) Trypsin — 0.53 mM EDTA were purchased from American Type Culture Collection (Manassas, VA). A Radio Immunoprecipitation Assay (RIPA) buffer was purchased from Santa Cruz Biotechnology (Santa Cruz, CA). An RNeasy Mini Kit extraction kit was purchased from Qiagen Sciences (MD, USA). All other chemicals were purchased from Sigma unless otherwise specified.

2.2. Bean sample preparation

The dry common bean seeds were cooked according to a previously reported method (Aparicio-Fernandez, Manzo-Bonilla, & Loarca-Piña, 2005). Briefly, the beans were placed in a beaker with HPLC-grade water (1:5 w/v) and heated at 90 °C ± 3 °C for 2.5 h or until the seeds were soft enough for consumption. The cooked seeds and broth were ground in a domestic grinder (Osterizer, Mexico), lyophilized, and stored in 50 mL centrifuge tubes at 4 °C until use.

2.3. Extraction of the non-digestible fraction

NDF was extracted following the previously reported procedure (Saura-Calixto, García-Alonso, Goñí, & Bravo, 2000). 300 mg of the samples treated as described above were incubated with pepsin (300 mg/mL, Sigma-Aldrich P7000) and porcine pancreatic α-amylase (120 mg/mL Sigma-Aldrich A3176). The samples were centrifuged (3000 × *g*, 15 min) and the supernatant were taken. The residue (insoluble NDF) was dried at 60 °C. Soluble NDF was obtained by dialyzing supernatants against water (25 °C, 48 h, water flow 7 L/h) (cellulose dialysis membranes, 12,000–14,000 MWCO; Sigma-Aldrich). The soluble and insoluble NDF were combined and lyophilized before protein extraction.

2.4. Preparation of common bean NDF peptide extract

Common bean protein extracts were produced as described previously (Pedroche et al., 2002) with minor modifications. Briefly, ten grams of lyophilized NDF was suspended in 100 mL of 0.2% NaOH solution pH 12, and stirred for 1 h. The solution was centrifuged at 8000 × *g* for 20 min; two additional extractions were carried out with half of the volume of NaOH solution. The pH of the supernatant was adjusted to 4.4 and the precipitate formed was recovered by centrifugation at 8000 × *g* for 20 min. The precipitate was washed with distilled water, cold saturated ammonium acetate in methanol, methanol, acetone and water again, and then it was lyophilized. In vitro simulated digestion of protein isolate was performed as reported previously (Megías et al., 2009) with minor modifications. Protein isolate was suspended in water (1:20 w/v); a sequential enzyme digestion was performed with pepsin (1:20 w/w, EC 3.4.23.1, Sigma-Aldrich P7000) and pancreatin (1:20 w/w, a mixture of several digestive enzymes produced by the exocrine cells of the porcine pancreas, EC 232-468-9, Sigma-Aldrich P7545) at 37 °C for 1.5 h for each enzyme. The hydrolysis was stopped by incubating at 75 °C for 20 min, the suspension was centrifuged at 20,000 × *g* for 15 min at 4 °C, and the supernatant was desalted through electro-dialysis using ElectroPrep System (Harvard Apparatus, Hill Road, MA) with 500 Da dialysis membrane. After desalting, the samples were lyophilized and kept at −20 °C until further use. Lyophilized material was called NDF peptide extract of AH-PE and BM-PE common bean cultivars. Later, the extracts were analyzed by using an UltrafleXtreme MALDI TOF/TOF mass spectrometer (Bruker Daltonics, Bremen, Germany) equipped with a frequency tripled Nd:YAG solid state laser using a FlexControl 1.4 software package (Bruker Daltonics). MS/MS analysis of each ion of interest was performed at 500 Hz in LIFT mode using a randomized raster, summed, and saved for analysis. Data processing was performed using a FlexAnalysis 3.4 software package (Bruker Daltonics, Bremen, Germany) and Biotools 3.2 (Bruker Daltonics, Bremen, Germany).

2.5. Cell culture and extraction of RNA

Human colon cancer cells HCT116 and RKO were cultured in Eagle's Minimum Essential Medium containing 10% FBS, 1% penicillin/streptomycin and 1% sodium pyruvate at 37 °C in 5% CO_2/95% air. Two hundred thousand cells per well were seeded in a 6-well plate and the total volume was adjusted to 2 mL with growth medium. The cells were allowed to grow for 24 h at 37 °C in 5% CO_2/95% air and treated with 0.5 mg/mL of AH-PE and BM-PE respectively for 24 h. A dose–response analysis with the peptide extracts was carried out where the IC_{50} values were obtained for each bean cultivar. Based on this preliminary information (data not shown), 0.5 mg/mL for the differential gene expression study was used.

Total RNA extraction was performed from treated and untreated cells using RNeasy Mini Kit (Qiagen, MD, USA) following the manufacturer's protocol. Concentration of RNA in the extract was determined using an ND-1000 spectrophotometer (NanoDrop Technologies, DE, USA). RNA quality was determined by the W. M. Keck Center for comparative and functional genomics in the Roy J. Carver Biotechnology Center at the University of Illinois at Urbana–Champaign using a Bioanalyzer 2100 and 2100 Expert Software Version B.02.06 (Agilent Technologies, CA, USA).

2.6. cDNA preparation and array hybridization

For microarray analysis, samples were prepared and analyzed by the W. M. Keck Center for Comparative and Functional Genomics in the Roy J. Carver Biotechnology Center at the University of Illinois at Urbana–Champaign. Total RNA were amplified and labeled with Cyanine 3- (Cy3-) and Cyanine 5- (Cy5-) as instructed by the manufacturer of the Agilent Low Input Quick Amp Labeling Kit, two-color (Agilent Technologies, CA, USA). Briefly, 200 ng of high quality total RNA was reverse

transcripted to double-strand cDNA using a poly dT-T7 promoter primer. The primer, template RNA, and quality-control transcripts of known concentration and quality were then denatured at 65 °C for 10 min and incubated for 2 h at 40 °C with 5× First-Strand Buffer, 0.1 M DTT, 10 mM dNTP mix, and Affinity Script RNase Block Mix. The Affinity Script enzyme was inactivated at 70 °C for 15 min. The resulting cDNA products were then used as templates for in vitro transcription master mix in the presence of T7 RNA polymerase and Cy3- and Cy5- labeled CTP and incubated at 40 °C for 2 h. Labeled cRNAs were purified using Qiagen's RNeasy Mini spin columns and eluted in 30 μL of nuclease-free water. After amplification and labeling, cRNA quantity and cyanine incorporation were determined using a NanoDrop ND-1000 (NanoDrop Technologies, DE, USA) and a Bioanalyzer 2100 with 2100 Expert software Version B.02.06 (Agilent Technologies, CA, USA). For each hybridization, 2.5 μg of Cy3- and Cy5-labeled cRNA was fragmented and hybridized onto an Agilent Human Gene Expression 4 × 44 K v2 Microarray for 17 h at 65 °C. After washing, the microarrays were scanned using an Agilent DNA microarray scanner. The intensity values of each scanned feature were quantified using an Agilent Feature Extraction software (version 10.73.1).

2.7. Microarray data analysis

Microarray data pre-processing and statistical analyses were done in R (R Development Core Team, 2013) (v3.0.1) using a limma package (Smyth, 2009) (v3.16.7). Median foreground and median background values from the arrays were read into R and any spots that had been manually flagged (−100 values) were given a weight of zero (Smyth & Speed, 2003). The background values were ignored as it added more noise to the data.

The individual Cy3- and Cy5- values from each array were all normalized together using a quantile method and then log 2-transformed. Agilent Human Gene Expression 4 × 44 K v2 Microarray interrogates 27,958 genes using 33,128 probes were spotted one time (1×) and 999 probes were spotted ten times (10×) each. Correlations between the replicate spots per probe were high and so the replicate spot values were simply averaged for each sample. The positive and negative control probes were used to assess what minimum expression level could be considered "detectable above background noise" (6 on the log 2 scale) and then the control probes were discarded. QC analyses indicated that a few of the samples had some slight quality issues, but not enough to be considered outliers. Therefore, quality weights (Ritchie et al., 2006) were estimated for each sample for use in the statistical model to down-weigh the lower quality arrays.

A mixed effects statistical model (Smyth, 2004) was fit on the 34,127 unique probes to estimate the mean expression level for each of the 6 cell line × treatment groups while accounting for dye effects, correlations due to array (Smyth, Michaud, & Scott, 2005) and sample quality weights. After fitting the model, 10,659 probes that did not have the expression values >6 in at least 2/16 samples were discarded. Pairwise comparisons between the peptide extract cultivars and control treatments within each cell line were pulled as contrasts from the model; one-way ANOVA was performed for pairwise comparison of results between the treated peptide extracts within each cell line and control cells. Raw *p*-values were adjusted separately for each comparison using the False Discovery Rate method (Benjamini & Hochberg, 1995). Gene annotation for each probe, including Gene Ontology terms and KEGG pathways, were taken from an HsAgilentDesign026652.db_2.9.0 package maintained by Bioconductor (Gentleman et al., 2004).

2.8. Functional enrichment and pathway analysis

The cut-off used for reporting significant changed in gene expression was FDR *p*-value <0.05 for HCT116 and RKO cell lines with both AH-PE and BM-PE treatments. Similarities and differences on the genes affected by AH-PE and BM-PE treatments were analyzed by GeneVenn (Pirooznia, Nagarajan, & Deng, 2007). The genes were annotated and biological processes were analyzed using DAVID v6.7 (Huang, Sherman, & Lempicki, 2009a, 2009b). Huang et al. (2009b) recommended that the *p*-value default cut-off was 0.1 in order to examine the significance of gene-term enrichment with a modified Fisher's exact test (EASE score). An enrichment score for each set of grouped genes was also determined. This is used to rank the overall importance or enrichment of the gene groups. It is the geometric mean of all the enrichment *p*-values for each annotation term associated with the gene members in the group. To emphasize that the geometric mean is a relative score instead of an absolute *p*-value, minus log transformation is applied on the average *p*-values; the higher score for a group indicates that the gene members in the group are involved in more enriched terms in a given study. The enrichment score of 1.3 is equivalent to a non-log scale of 0.05.

As an alternative approach to identify the biological processes and functions that are modulated after exposure to AH-PE and BM-PE, an exploratory functional analysis was performed using IPA v9.0 [Ingenuity® Systems]. Core analysis parameters were set-up as follows: Network analysis: direct and indirect relationship; Molecules per network: 35; Network per analysis: 25; Data sources: all; Confidence: experimentally observed; Species: human; and Tissues and cell lines: all. Additionally, Downstream Effect Analysis was performed using IPA, which identifies biological functions that are expected to be increased/decreased given the observed gene expression changed in a data-set uploaded to the software; in order to reduce the chance that random data will generate significant predictions, an absolute z-score of ≥2 was considered significant, thus, in this case, a function is decreased if the z-score ≤ 2, and increased if the z-score ≥ 2

2.9. Quantitative RT-PCR

RNA expression of selected genes was measured using a real-time quantitative PCR using Primetime qPCR from Integrated DNA Technologies (California, USA). Briefly, 2 μg purified RNA was reverse transcribed into complementary DNA using a high capacity DNA archive kit from Applied Biosystems (California, USA). The PCR components mixes were then prepared by combining each cDNA sample with Primetime qPCR Gene Expression Assay, Primetime qPCR Gene Expression Master Mix, and RNase-free water. Mixes were then plated in a 384-well plate and gene expression was determined using 7900HT Real-Time PCR System (Applied Biosystems, CA, USA). Cycling conditions were 2 min at 50 °C for 1 cycle, then 10 min at 95 °C for 1 cycle followed by 15 s at 95 °C and 1 min at 60 °C for 40 cycles. The gene expression was quantified using the ΔΔCt method and fold-change values were reported as $2^{-(\Delta\Delta Ct)}$. The relative amount of each target gene was normalized to GAPDH. All reactions were carried out in triplicate to confirm reproducibility. The following primers were used in the RT-PCR analysis.

Gene	Sense (5–3)	Antisense (5–3)
OSGIN1	CTTCGTGTAGGGTGTGTAGC	CCATGAGCTCCCCAGAAAG
PDE4B	GTCTATTGTGAGAATATCCAGCCA	TCACGCTTTGGAGTCAACA
MAGEA2	GATCTTCTCCTTCAATGCTCCT	GATGCAGTGGTTCTAGGATCTG
EEF1A2	CACCCAGGCATACTTGAAGG	GCCACCTCATCTCCAAATGC
KRT19	TTGGTTCGGAAGTCATCTGC	AGCCACTACTACACGACCAT
JUN	GGTTTCAGGAGTTTGTAGTCGT	CGGATGTGCACTAAAATGGAAC

3. Results

3.1. Common bean peptide extracts characterization

A MALDI-TOF analysis (Fig. 1) resulted in profiles of around 17 peptides ranging from 505 to 1019 kDa, with slight differences among percentages of abundance in each cultivar. Five peptides represented

70% of the total proteins in both AH-PE and BM-PE (GLTSK, LSGNK, GEGSGA, MPACGSS and MTEEY).

3.2. Effect of AH-PE and BM-PE on gene expression profile of HCT116 and RKO human colon cancer cells

Fig. 2 shows the Venn diagram comparing the number of DEGs between the cultivars per cell line. Within the full list of the represented genes in the microarray, 511 and 964 DEGs were found for AH-PE and BM-PE, respectively, in HCT116 cells, sharing 405 common DEGs among the cultivars. In contrast, 45 and 32 DEGs were found for AH-PE and BM-PE, respectively, in RKO cells, sharing 19 common DEGs in both cultivars. Also, it was found that among these DEGs, the differential expression of only 8 genes in both cell lines was commonly triggered by both bean cultivars, namely C11orf31, C9orf169, EMP1, GEM, PLIN2, SUN3, TRIM16L and TXNRD1.

Supplementary Tables 1 and 2 list the DEGs in HCT116 cell line in response to AH-PE and BM-PE, respectively. Supplementary Tables 3 and 4 list the DEGs in RKO cell line in response to AH-PE and BM-PE, respectively.

3.3. Annotation and functional enrichment analysis of HCT116 genes affected by AH-PE

Treatment of 0.5 mg/mL AH-PE cultivar resulted in significantly different expressions of 511 genes in HCT116 human colon cancer cells as compared to the control (water-treated). Analysis of this set of genes using DAVID showed that 473 genes were recognized by this bioinformatics tool. Using functional annotation clustering, 159 clusters were generated of which 10 clusters had an enrichment score of greater than or equal to 1.3 ($p < 0.05$). Table 1 shows the highly-enriched cluster with enrichment score of at least 2.0. These highly-enriched clusters are associated with a basic-leucine zipper transcription factor (bZIP), insoluble fraction, oxidation–reduction reaction and protein phosphatases. Other significantly-enriched clusters included genes associated with oxidoreductase activity, nucleus, DNA binding and transcription factor activity, chromosome organization, microsome, endoplasmic reticulum membrane and organelle membrane, cofactor metabolic process and regulation of microtubule polymerization or depolymerization. The oxidation–reduction cluster contained one of the most numbers of genes with 34 genes on the list of 473 genes recognized by DAVID and the fold changes and their corresponding P-value are shown in Table 2.

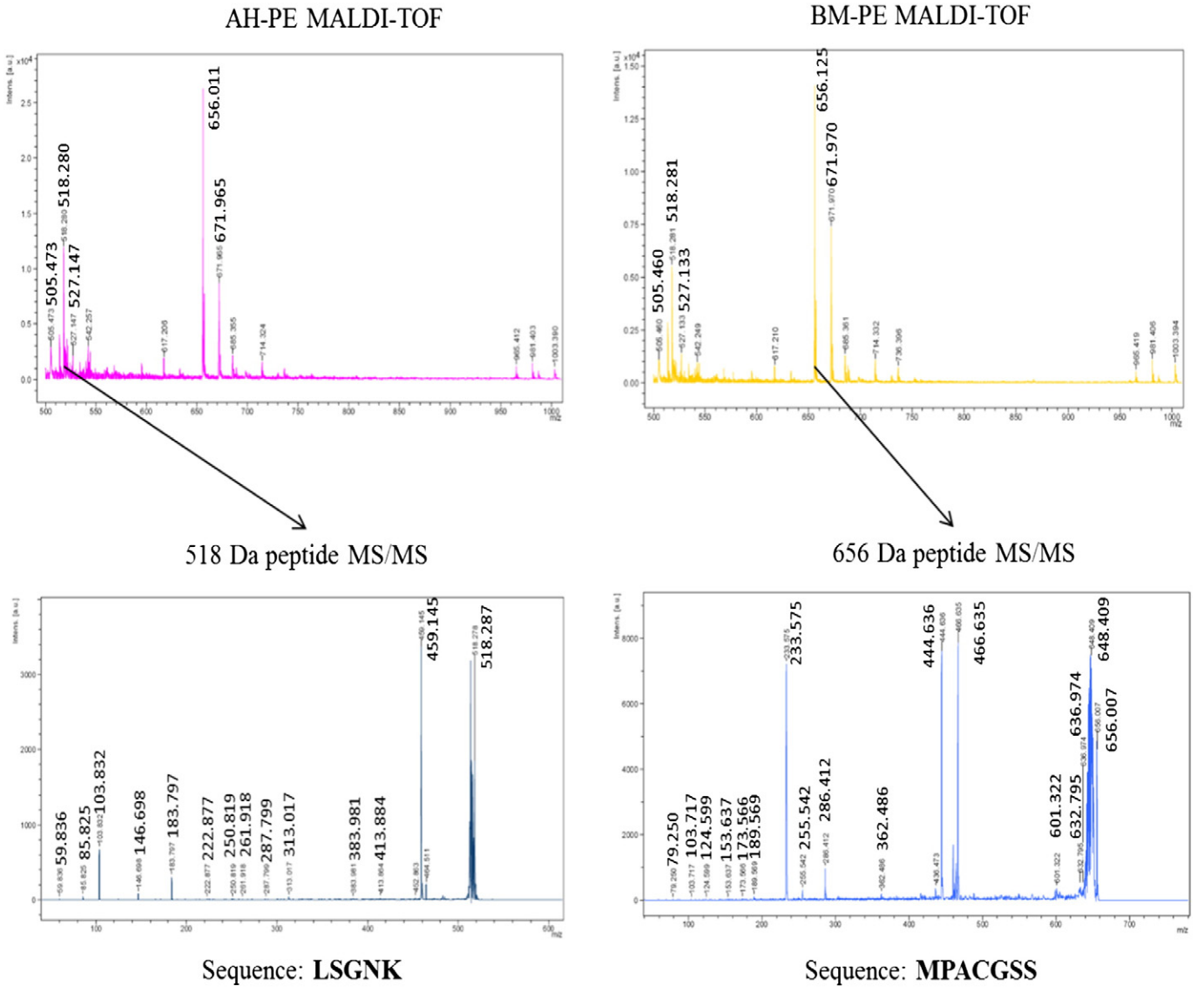

Fig. 1. Schematic diagram showing the identification of peptides from the peptide extracts which were subjected to MALDI-TOF and those ions having more than 5% area were subjected to MS–MS analysis for sequence identification. Examples for peptides LSGNK and MPACGSS are presented.

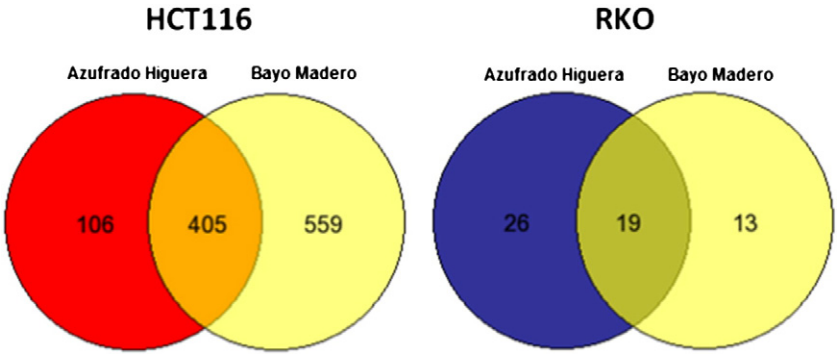

Fig. 2. Venn diagram of the overlap DEGs in response to cultivars per cell line, HCT116 and RKO treated with 0.5 mg/mL AH-PE and 0.5 mg/mL BM-PE, as determined by GeneVenn.

Table 1
Highly-enriched cluster in genes affected by AH-PE and BM-PE treatments in HCT116 human colon cancer cells.

Term	ES[a]	Count	*p*-value
AH-PE[b]			
Annotation cluster 1	3.11		
Domain: leucine-zipper		10	0.001
DNA-binding region: Basic motif		11	0.005
Annotation cluster 2	3.04		
Insoluble fraction		36	0.000
Cell fraction		43	0.000
Membrane fraction		34	0.000
Vesicular fraction		13	0.000
Annotation cluster 3	2.48		
Oxidation-reduction		34	0.000
Oxidoreductase		30	0.000
Coenzyme binding		14	0.001
FAD		10	0.002
Cofactor binding		16	0.002
Annotation cluster 4	2.29		
Protein phosphatase		10	0.004
Protein amino acid dephosphorylation		10	0.005
Phosphoprotein phosphatase activity		11	0.009
Phosphatase activity		14	0.010
Dephosphorylation		10	0.012
MAPK signaling pathway		12	0.047
BM-PE[c]			
Annotation cluster 1	4.96		
Oxidoreductase		49	0.000
Oxidation reduction		53	0.000
NADP		19	0.000
Annotation cluster 2	3.25		
Basic-leucine zipper (bZIP) transcription factor		12	0.000
BRLZ		12	0.000
Domain: Leucine-zipper		16	0.000
DNA-binding region: basic motif		18	0.000
Sequence-specific DNA binding		34	0.012
Annotation cluster 3	3.14		
Cellular response to extracellular stimulus		13	0.000
Response to extracellular stimulus		21	0.002
Response to nutrient levels		17	0.012
Annotation cluster 4	3.08		
Protein phosphatase		19	0.000
Dephosphorylation		21	0.000
Phosphoprotein phosphatase activity		22	0.000
Phosphatase activity		28	0.000
Protein amino acid Dephosphorylation		19	0.000
Protein tyrosine phosphatase activity		15	0.000
Domain: tyrosine–protein phosphatase		11	0.000
Active site: phosphocysteine intermediate		12	0.001
Protein–tyrosine phosphatase		12	0.001
Dual-specific/protein–tyrosine phosphatase, conserved reg		12	0.001
Protein–tyrosine phosphatase, active site		12	0.002

[a] ES—enrichment score.
[b] Highly-enriched cluster with enrichment score of at least 2. For each annotation cluster reported, only terms with at least 10 genes (count) are specified.
[c] Highly-enriched cluster with enrichment score of at least 3. For each annotation cluster reported, only terms with at least 10 genes (count) are specified.

DAVID pathway finder showed that KEGG pathway identified 2 records associated with MAPK signaling pathway and fatty acid metabolism. BIOCARTA also identified 2 pathways associated to regulation of MAP kinase pathways through dual specificity phosphatases and mitochondrial carnitine palmitoyltransferase (CPT) system. Supplemental Fig. 1 shows the genes affected in MAPK signaling pathway as adapted from KEGG.

3.4. Annotation and functional enrichment analysis of HCT116 genes affected by BM-PE

Treatment of 0.5 mg/mL NDF-PE from BM cultivar resulted in the significantly different expression of 964 genes of which 822 were recognized by DAVID. A functional annotation clustering tool resulted in 244 clusters of which 29 clusters had enrichment score of at least 1.3 ($P < 0.05$). These clusters included terms such as oxidoreductase, bZIP, cellular response to extracellular stimulus, protein phosphatase, NADP or NAPDH binding, response to organic substance, cell redox homeostasis, negative regulation of transcription activity, regulation of apoptosis, blood vessel morphogenesis, mitochondrion, microsome, cofactor metabolic process, nucleoside-triphosphatase regulator activity, cell migration, enzyme linked receptor protein signaling, small GTPase binding, plectrins homology, protein dimerization activity, negative regulation of molecular function, protein tetramerization, response to oxidative stress, regulation of Cdc42 protein signal transduction, cytoskeleton organization and steroid metabolic process. Some of the terms associated with the clusters with an enrichment score of at least 3.0 and 10 genes significantly affected are listed in Table 1; while the genes associated with response to cellular stimulus are shown in Table 3. In addition, KEGG pathway identified 17 chart records including MAPK signaling pathway with 22 genes; butanoate metabolism with 6 genes; Wnt signaling pathway with 14 genes; bladder cancer with 6 genes; focal adhesion with 16 genes; TGF-β signaling pathway with 9 genes; apoptosis with 9 genes; glycolysis/gluconeogenesis with 7 genes; adherence junction with 8 genes; fructose and mannose metabolism with 5 genes; regulation of actin cytoskeleton with 16 genes; pathways in cancer with 22 genes; GnRH signaling pathway with 9 genes; CRC with 8 genes; epithelial cell signaling in *Helicobacter pylori* infection with 7 genes; arginine and proline metabolism with 6 genes and amyotrophic lateral sclerosis with 6 genes. Supplemental Fig. 2 shows the adapted pathway from KEGG using the genes affected in pathways in cancer record. On the other hand, BIOCARTA identified 10 chart records including oxidative stress induced gene expression via Nrf2, MAP kinase inactivation of SMRT corepressor, NF-κB activation by nontypeable *Haemophilus influenzae*, mCalpain and friends in cell motility, links between Pyk2 and MAP kinases, keratinocyte differentiation, angiotensin II mediated activation of JNK pathway via Pyk2 dependent signaling, SREBP control of lipid synthesis, free radical induced apoptosis and regulation of MAP kinase pathway through dual specificity phosphatases.

Table 2
Changes in the gene expression of HCT116 human colon cancer cells associated with oxidation–reduction reaction as affected by AH-PE treatment.

Gene symbol	Description	Entrez gene ID	Fold change	FDR *p*-value
AKR1B10	Aldo-keto reductase family 1, member B10 (aldose reductase)	57,106	+2.5	0.001
TXNRD1	Thioredoxin reductase 1; hypothetical LOC100130902	7296	+2.2	0.001
SRXN1	Sulfiredoxin 1 homolog (*S. cerevisiae*)	140,809	+2.2	0.001
FTL	Ferritin, light polypeptide	2512	+2.0	0.006
CYP4F11	Cytochrome P450, family 4, subfamily F, polypeptide 11	57,834	+1.9	0.000
NQO1	NAD(P)H dehydrogenase, quinone 1	1728	+1.9	0.001
ALDH1A3	Aldehyde dehydrogenase 1 family, member A3	220	+1.8	0.016
GSR	Glutathione reductase	2936	+1.7	0.001
CYP4F8	Cytochrome P450, family 4, subfamily F, polypeptide 8	11,283	+1.7	0.003
CYP4F12	Cytochrome P450, family 4, subfamily F, polypeptide 12	66,002	+1.7	0.015
LDHC	Lactate dehydrogenase C	3948	+1.6	0.016
AIFM2	Apoptosis-inducing factor, mitochondrion-associated 2	84,883	+1.5	0.001
ASPH	Aspartate beta-hydroxylase	444	+1.5	0.015
CYB5A	Cytochrome b5 type A (microsomal)	1528	+1.5	0.022
STEAP1	Six transmembrane epithelial antigen of the prostate 1	26,872	+1.5	0.041
GPD1L	Glycerol-3-phosphate dehydrogenase 1-like	23,171	+1.4	0.031
SQLE	Squalene epoxidase	6713	+1.4	0.033
MSMO	Sterol-C4-methyl oxidase-like	6307	+1.4	0.036
GFOD1	Glucose–fructose oxidoreductase domain containing 1	54,438	+1.4	0.048
CYP4F2	Cytochrome P450, family 4, subfamily F, polypeptide 2	8529	+1.3	0.000
QSOX2	Quiescin Q6 sulfhydryl oxidase 2	169,714	+1.3	0.036
ALDH7A1	Aldehyde dehydrogenase 7 family, member A1	501	−1.3	0.000
MTHDF2	Methylenetetrahydrofolate dehydrogenase (NADP + dependent) 2	10,797	−1.4	0.033
TMX1	Thioredoxin-related transmembrane protein 1	81,542	−1.4	0.033
DHFR	Dihydrofolate reductase	1719	−1.5	0.015
GPX8	Glutathione peroxidase 8 (putative)	493,869	−1.5	0.020
HADH	Hydroxyacyl-coenzyme A dehydrogenase	3033	−1.5	0.041
DHFRL1	Dihydrofolate reductase like 1	200,895	−1.5	0.045
ACOX2	Acyl-coenzyme A oxidase 2, branched chain	8309	−1.6	0.000
ALDH6A1	Aldehyde dehydrogenase 6 family, member A1	4329	−1.7	0.015
TP53I3	Tumor protein p53 inducible protein 3	9540	−1.9	0.007
DHRS2	Dehydrogenase/reductase (SDR family) member 2	10,202	−2.3	0.047

The significance in expression of genes was considered according to a False Discovery Rate (FDR) adjusted *p*-value <0.05.

3.5. Annotation and functional enrichment analysis of RKO genes affected by AH-PE

At 0.5 mg/mL, AH-PE affected 45 genes on RKO human colon cancer cells. DAVID recognized 36 genes and the functional annotation clustering tool of this set of genes led to 10 annotation clusters with 2 clusters having an enrichment score of at least 1.3 ($P < 0.05$). These clusters contained terms associated with the response to inorganic substance, response to hormone stimulus and response to wounding as listed in Table 4. KEGG pathway and BIOCARTA did not recognize any chart record from the 36 genes recognized by DAVID.

3.6. Annotation and functional enrichment analysis of RKO genes affected by BM-PE

Only 32 genes in RKO human colon cancer cells were significantly affected by the BM-PE treatment at 0.5 mg/mL. Out of 32 genes, 28 genes were recognized by DAVID and the functional annotation clustering tool

Table 3
Changes in the gene expression of HCT116 human colon cancer cells associated with oxidation–reduction reaction as affected by BM-PE treatment.

Gene symbol	Description	Entrez gene ID	Fold change	FDR *p*-value
JUN	Jun oncogene	3725	+3.8	0.000
FOSL1	FOS-like antigen 1	8061	+3.1	0.025
ADM	Adrenomedullin	133	+2.3	0.008
DUSP1	Dual specificity phosphatase 1	1843	+2.1	0.005
HMOX1	Heme oxygenase (decycling) 1	3162	+2.1	0.010
AXL	AXL receptor tyrosine kinase	558	+2.0	0.001
ADORA2B	Hypothetical LOC100131909; adenosine A2b receptor	136	+1.6	0.008
ATG12	ATG12 autophagy related 12 homolog (*S. cerevisiae*)	9140	+1.6	0.009
PDGFA	Platelet-derived growth factor alpha polypeptide	5154	+1.6	0.025
ITGA6	Integrin, alpha 6	3655	+1.5	0.013
ATG16L1	ATG16 autophagy related 16-like 1 (*S. cerevisiae*)	55,054	+1.4	0.040
CAV1	Caveolin 1, caveolae protein, 22 kDa	857	+1.4	0.041
RARA	Retinoic acid receptor, alpha	5914	+1.4	0.045
HSD11B2	Hydroxysteroid (11-β) dehydrogenase 2	3291	+1.4	0.050
DDIT3	DNA-damage-inducible transcript 3	1649	−1.3	0.020
CPS1	Carbamoyl-phosphate synthetase 1, mitochondrial	1373	−1.4	0.042
TP53	Tumor protein p53	7157	−1.5	0.013
CYP24A1	Cytochrome P450, family 24, subfamily A, polypeptide 1	1591	−1.5	0.032
HFE	Hemochromatosis	3077	−1.6	0.020
DDAH2	Dimethylarginine dimethylaminohydrolase 2	23,564	−1.7	0.047
SREBF1	Sterol regulatory element binding transcription factor 1	6720	−1.8	0.039

The significance in expression of genes was considered according to a False Discovery Rate (FDR) adjusted *p*-value < 0.05.

Table 4
Highly-enriched cluster in genes affected by AH-PE and BM-PE treatments in RKO human colon cancer cells.

Term	ES*	Count	*p*-value
AH-PE			
Annotation cluster 1	1.31		
Response to inorganic substance		5	0.000
Response to hormone stimulus		4	0.023
Response to endogenous stimulus		4	0.030
Response to organic substance		5	0.032
Response to steroid hormone stimulus		3	0.042
Annotation cluster 2	1.31		
Response to wounding		5	0.011
Inflammatory response		4	0.017
BM-PE			
Annotation cluster 1	2.50		
Selenium binding		3	0.000
Selenocysteine		3	0.001
Selenium		3	0.001
Homeostatic process		6	0.002
Cell redox homeostasis		3	0.003
Cellular homeostasis		4	0.019
Annotation cluster 2	1.38		
Response to wounding		5	0.004
Cell proliferation		4	0.016
Annotation cluster 3	1.34		
Response to organic substance		5	0.011
Extracellular region part		5	0.034

* ES—enrichment score.

led to 9 annotation clusters of which 3 clusters had the enrichment score of at least 1.3 ($P < 0.05$). These clusters included terms associated with selenium binding, response to wounding and response to organic substance. The list of terms for each of the significantly annotated clusters is presented in Table 4. KEGG pathway identified one chart record pertaining to glutathione metabolism with 2 genes significantly affected namely glutathione peroxidase 1 and glutathione S-transferase kappa 1.

3.7. Annotation and functional enrichment analysis of genes significantly affected by both AH-PE and BM-PE in HCT116 and RKO colon cancer cells

Since only eight DEGs were common in HCT116 and RKO cell lines with both AH-PE and BM-PE treatments, we decided to analyze the association of common DEGs on cultivar per cell line. We first determined by DAVID the association of 405 common DEGs for AH-PE and BM-PE in HCT116 cell line, showing that treatments affected genes related to oxidation–reduction, bZIP transcription factor, coenzyme binding, protein dimerization activity and regulation of apoptosis. The association of DEGs for each treatment in HCT116 cell line was also evaluated and the highest enrichment scores were considered. Genes modified for AH-PE were related to bZIP domain transcription factors, sequence-specific DNA binding, oxidation reduction, coenzyme binding and MAPK phosphatase; as for BM-PE the highest enriched scores corresponded to oxidation reduction, bZIP transcription factors, response to extracellular stimulus, response to starvation and response to nutrient levels (Table 5).

Moreover, RKO cell line showed to be affected in the same biological processes by both AH-PE and BM-PE treatments, even for the common DEGs among cultivars; being the highest enrichment scored cell redox homeostasis, homeostatic process, glutathione metabolic process, peptide metabolic process and coenzyme metabolic process (Table 5).

3.8. Analysis of genes significantly affected by AH-PE and BM-PE in HCT116 and RKO colon cancer cells by Ingenuity Pathway Analysis

Another bioinformatics approach used to identify biological processes affected by AH-PE and BM-PE was IPA. Further enrichment analysis on canonical pathways of IPA Knowledge Base provided significant overlaid pathways through the list of DEGs, finding for both cell lines the potential activation of oxidative stress-related pathways, of which highlight the highest scored in RKO cells glutathione redox reactions I. For HCT116 cell line NRF2-mediated oxidative stress response as some of the main effects derived from the treatment of cell lines with AH-PE and BM-PE (Fig. 3A).

Analysis of HCT116 cell line suggested that AH-PE and BM-PE exerted the response of detoxifying and xenobiotic metabolism effects by the activation of NRF2-mediated oxidative stress response signaling pathway identified with IPA. Examination of downstream targets of NRF2 evidenced transcriptional NRF2-mediated induction of several enzymes in detoxifying metabolism, such as heme oxygenase 1 (HMOX), cytoplasmic pyridine nucleotide oxidoreductase (TRXR1), glutathione reductase (GSR) and superoxide dismutase (SOD). Also, associated with this pathway the transcript level of phase III transporter MRP2 was increased. About the upstream modified transcript levels on NRF2

Table 5
The highest enrichment scored biological functions gene sets of HCT116 and RKO cell lines affected by the common bean NDF peptide extracts determined by DAVID and downstream effect analysis global results, determined by IPA®.

Cell line/cultivar	Biological function	Count	*p*-Value*	Enrichment score
HCT116				
AH/BM-PE	Oxidation reduction	27	2.5E−4	2.96
	Basic-leucine zipper (bZIP) transcription factor	8	5.1E−5	2.74
	Coenzyme binding	11	3.8E−3	1.67
	Protein dimerization activity	23	1.5E−3	1.35
	Regulation of apoptosis	26	0.012	1.19
RKO				
AH/BM-PE	Cell redox homeostasis	4	2.7E−3	2.47
	Homeostatic process	8	0.048	1.52
	Glutathione metabolic process	3	6.8E−3	1.52
	Peptide metabolic process	3	0.023	1.52
	Coenzyme metabolic process	4	0.03	1.52
Cell line	**Biological function**	**Predicted activated state**	***p*-Value**	**z-Score**
HCT116	Cell death	Increase	3.99E−32	4.45
	Apoptosis	Increase	2.6E−35	4.02
	Cell death of tumor cell lines	Increase	2.7E−19	2.32
	Interphase of tumor cell lines	Decrease	2.56E−9	−2.21
	Hypertrophy	Decrease	1.04E−3	−2.07
	Hyperplasia of leukocytes	Decrease	1.01E−4	−2.00
RKO	Proliferation of tumor cell lines	Decrease	1.02E−9	−3.00
	G1/S phase in cell cycle	Decrease	7.38E−7	−2.42

* FDR-adjusted *p*-value.

function, it was observed a strong induction of genes encoding for members of activator protein 1 (AP-1) complex, such as JUN, and FRA1, as well as induction of genes encoding mitogen-activated protein kinases (MEK 1/2) and mitogen-activated protein kinase kinase kinases (3/4/6/7). On the other hand, analysis of genes affected by AH-PE and BM-PE in RKO cell line showed that the highest scored canonical pathway was glutathione redox reactions I; which overlapping with DEGs showed strong down-regulation of glutathione peroxidase 8 (GPX8), glutathione peroxidase 1 (GPX1), and GSR antioxidant enzymes.

Functional biological analysis using data-set containing common DEGs per cultivar of HCT116 identified significant represented molecular and cellular functions. These were related to cell death and survival, cell cycle, cellular growth and proliferation, connective tissue disorders and dermatological diseases and conditions for HCT116 cell line. Whereas for RKO those significant affected biological functions were cellular movement, cancer, reproductive system disease, tissue development and hematological system development and function (Fig. 3B). Additionally, a Downstream Effect Analysis was performed using IPA, which identified biological functions expected to be increased/decreased given the observed gene expression changed in a data-set uploaded to the software. In order to reduce the chance that random data will generate significant predictions, an absolute z-score of ≥ 2 was considered significant, thus, in this case, a function decreased if the z-score ≤ 2, and increased if the z-score ≥ 2. HCT116 cell line treated with AH-PE and BM-PE differential gene expression resulted in a high scored increase of cell death ($p = 3.99E-32$, z-score $= 4.45$), apoptosis ($p = 2.60E-35$, z-score $= 4.024$) and cell death of tumor cell lines ($p = 2.70E-19$, z-score $= 2.32$). On the other hand, the highest scored decrease was found in the interphase of tumor cell lines ($p = 2.56E-9$, z-score $= -2.21$), hypertrophy ($p = 1.04E-3$, z-score $= -2.078$) and hyperplasia of leukocytes ($p = 1.01E-4$, z-score $= -2.00$); whereas for RKO cell line treated with AH-PE and BM-PE it was predicted a significant decrease in proliferation of tumor cell lines ($p = 1.02E-9$, z-score $= -3.00$) and G1/S phase in cell cycle ($p = 7.38E-7$, z-score $= -2.42$) (Table 5).

In Fig. 4 the highly correlated network among DEGs in HCT116 treated with AH-PE and BM-PE cells and biological processes predicted regulations can be observed, being 56 DEG involved with the regulation of cell death, interphase of cell cycle, hypertrophy and hyperplasia. Moreover, in RKO cell line treated with AH-PE and BM-PE, 12 DEG were related to the regulation of proliferation of tumor cell lines and phase transition G1/S in cell cycle as shown in Fig. 5.

3.9. Validation of selected genes by RT-PCR

We selected genes that were highly affected by the peptide extracts for both human colon cancer cell lines for validation. For HCT116 cell line, we validated PDE4B, JUN and OSGIN by RT-PCR. As shown in

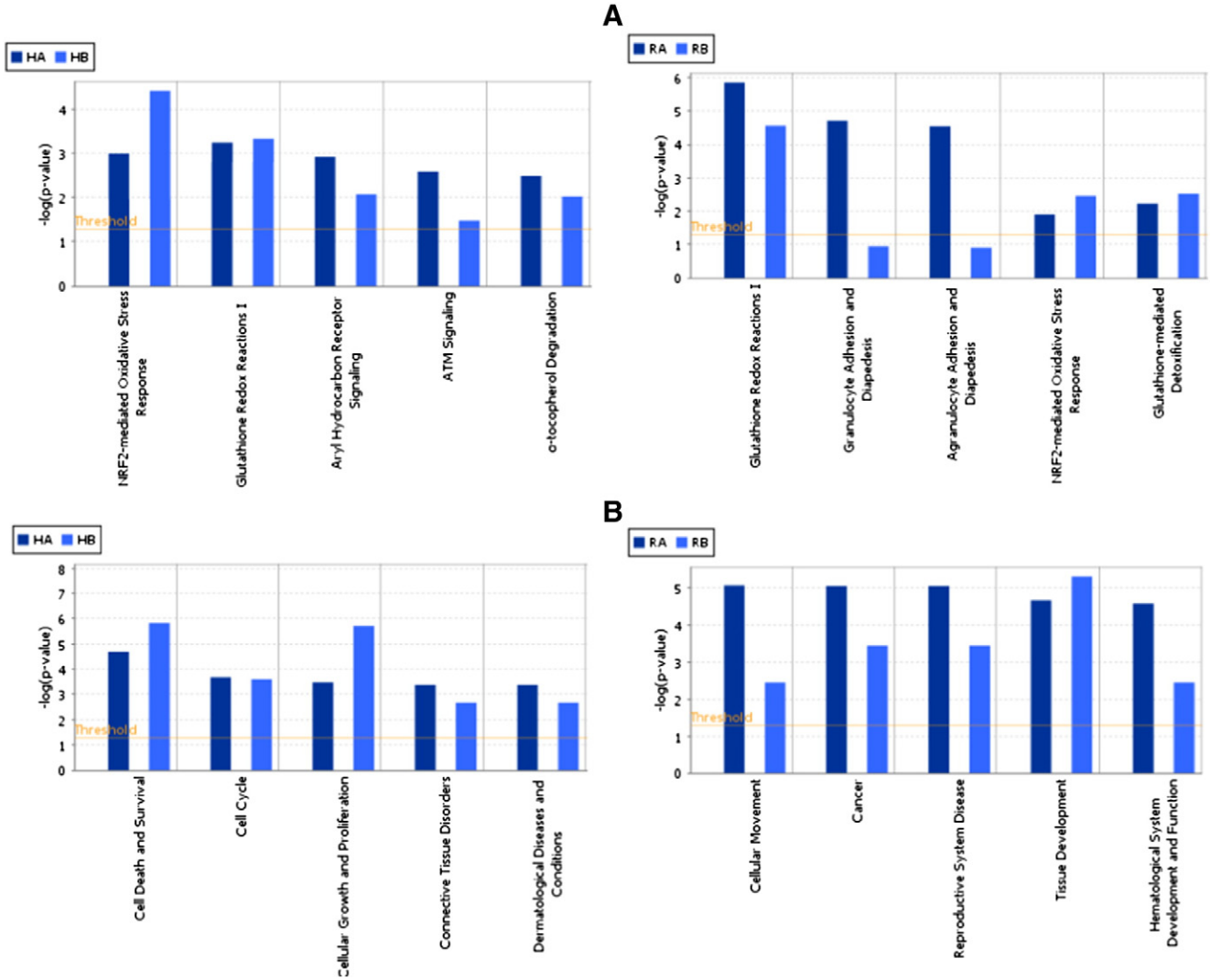

Fig. 3. Comparison of the canonical pathways A), and biological function B) among the genes affected by AH-PE and BM-PE treatment in both RKO and HCT116 cell lines.

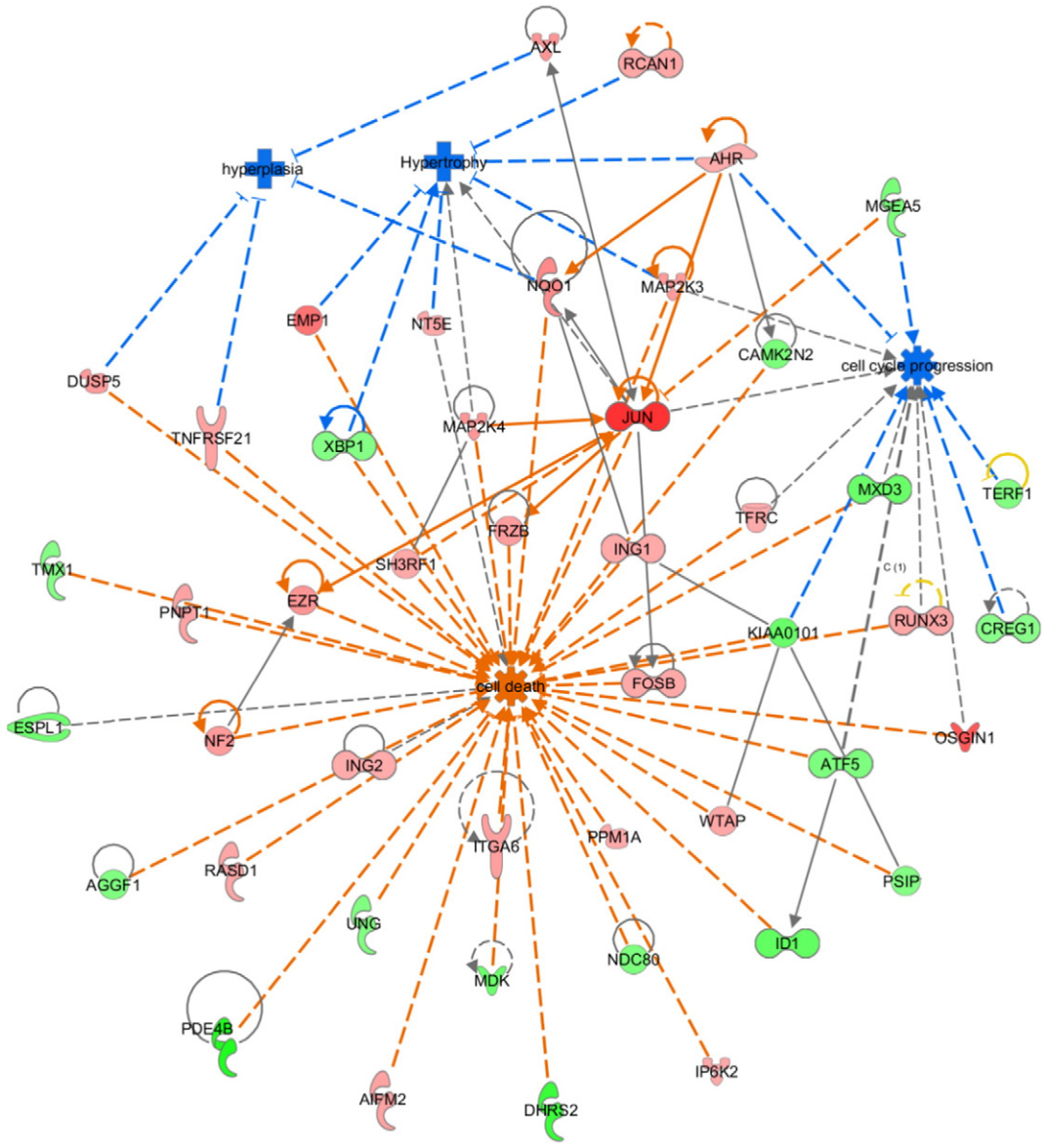

Fig. 4. Downstream effect analysis gene network obtained from IPA knowledge base illustrating interactions between DEGs and highest affected biological functions in HCT116 cell line in response to AH-PE and BM-PE. The type of interaction is indicated by orange color (prediction of increase in the event), in blue (prediction of decrease in the event) and gray (known to be related, but effect not predicted).

Table 6, a good agreement between the microarray and RT-PCR results for both common bean varieties was found. PDE4B was both downregulated by AH-PE (2.6-fold, microarray and 2.2-fold, RT-PCR) and BM-PE (2.5-fold, microarray and 2.4-fold, RT-PCR). On the other hand both JUN and OSGIN genes were upregulated by both cultivar peptide extracts. We selected KRT19, MAGEA2B and EEF1A2 for validation in case of RKO human colon cancer cell line. We only found the agreement between the microarray and RT-PCR results for the AH-PE-treated cells but not for the BM-PE-treated cells (Table 6).

4. Discussion

According to the microarray analysis, AH-PE and BM-PE shared 405 common DEGs when treated HCT116 cells and 19 common DEGs for RKO cells. Only 8 DEGs were common for both cell lines and both types of beans, indicating a markedly different expression profile comparing these human colon cancer cells.

Both bean cultivars caused differential expression on 8 genes in both cell lines (C11orf31, C9orf169, EMP1, GEM, PLIN2, SUN3, TRIM16L and TXNRD1). Two of them, TXNRD1 and C11orf31, are genes that encode for selenoproteins in response to oxidative stress. It has been hypothesized that some selenoproteins play important roles in the ability of colonic epithelial cells to respond to microbial and oxidative challenges and that low intake of selenium combined with low expression of the proteins can increase the risk of colonic pre-neoplastic lesions (Méplan & Hesketh, 2011). TXNRD1 was up-regulated and C11orf31 down-regulated in all cases. In the previous reports, it has been informed about the increase of the risk of CRC caused by polymorphisms in TXNRD1, and although C11orf31 is also a selenoprotein, it has not been associated with CRC through either main or interactive effects (Slattery, Lundgreen, Welbourn, Corcoran, & Wolff, 2012). Moreover, EMP 1 and PLIN2 were modestly up-regulated in all cases, these genes are considered to increase the risk of proliferation of colon cancer (Joyce, Cantarella, Isella, Medico, & Pintzas, 2009, Matsubara et al., 2011) and therefore, this modulation could be related to the aggressiveness of the cell lines. Regarding the remaining genes, this is one of the first reports to associate their modulation with effects in colon cancer; studies are undertaken to determine these genes in tissues from in vivo studies.

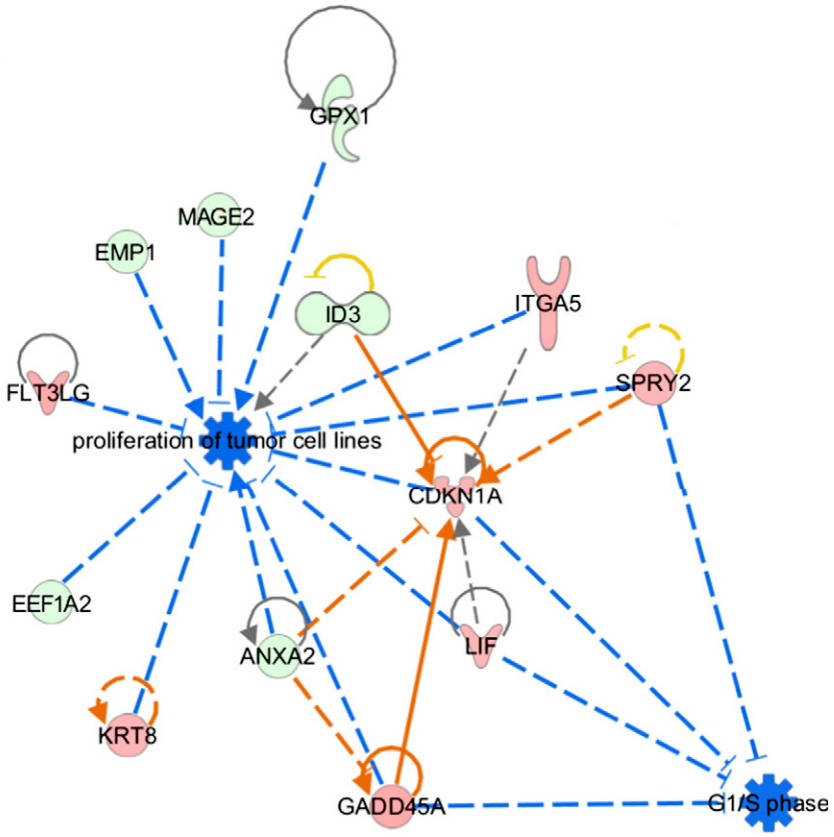

Fig. 5. Downstream effect analysis gene network obtained from IPA knowledge base illustrating interactions between DEGs and highest affected biological functions in RKO cell line in response to AH-PE and BM-PE. The type of interaction is indicated by orange color (prediction of increase in the event), in blue (prediction of decrease in the event), and gray (known to be related, but effect not predicted).

Regarding HCT116 cell line, the highest score overlapping with a specific canonical pathway was associated with the transcriptional activation of typical nuclear factor NRF2 target genes such as HMOX1, TRXR1 and FTL1. Interestingly, the expression of the oxidative stress induced growth inhibitor 1 (OSGIN1) was induced in this cell line. Although IPA did not include this gene in NRF2-mediated response to oxidative stress, the expression of OSGIN1 is known to follow similar expression pattern to that of HMOX1 in response to oxidative signals (Valdés et al., 2013). The encoded protein for OSGIN1 regulates apoptosis intrinsically by inducing cytochrome c release from mitochondria. It also appears to be a key regulator of anti-inflammatory molecules and the loss of this protein correlates with uncontrolled cell growth and tumor formation (Wang et al., 2005; Yao et al., 2006). Previously, it has been reported the potent antioxidant activity of the heme-derived metabolites generated by HMOX1 catalysis (biliverdin and bilirubin) and the cytoprotective actions of carbon monoxide on vascular endothelium and nerve cells. Therefore, it is widely accepted that induction of HMOX expression represents an adaptive response that increases cell resistance to oxidative injury (Valdés et al., 2013). NRF2 pathway plays an essential role in the antioxidant response elements (ARE) located in the upstream promoter region of many of the phase II antioxidant genes involved in xenobiotic metabolism and oxidative stress response. It is known that several food compounds that act as inducers of ARE-regulated gene expression provide chemopreventive effects (Lee & Surh, 2005).

HCT116 cell line did not show apoptosis canonical pathway regulation by either AH-PE or BM-PE but downstream effect analysis showed that apoptosis was the highest scored increased biological event. The

Table 6
Comparison of gene expression ratios in response to AH-PE and BM-PE treatment as determined by microarray analysis and RT-qPCR in colon cancer cell lines HCT116 and RKO.

Cultivar/gene	AH-PE				BM-PE			
	Microarray		qPCR		Microarray		qPCR	
	FC	FDR *p*-value	FC	*p*-Value	FC	FDR *p*-value	FC	*p*-Value
HCT116								
PDE4B	−2.6	3.9E−5	−2.2	0.0007	−2.5	1.1E−5	−2.4	0.0010
JUN	3.3	1.9E−3	1.1	0.5130	3.8	4.2E−4	1.1	0.1388
OSGIN1	2.7	5.7E−3	3.9	0.0287	3.6	4.3E−4	5.5	0.0010
RKO								
KRT19	−21.4	0.043	−1.7	0.0173	−11.1	0.017	1.6	0.3009
MAGEA2B	−3.8	0.010	−1.0	0.9857	−2.7	0.018	1.5	0.1940
EEF1A2	−7.5	0.013	−2.1	0.0001	−4.9	0.020	1.2	0.6416

The significance in expression of genes was considered according to a False Discovery Rate (FDR) adjusted p-value < 0.05.

activation of a cytoprotective response is related with the growth-hormone independent aggressiveness of HCT116 cell line (Awwad et al., 2003). However, it regulates a noteworthy number of networked genes related to cell death based on previous findings and association with molecules that eventually will lead to inhibition of cell survival. For instance, data revealed strong transcriptional induction of AP-1 members, JUN and FRA1 in response to AH-PE and BM-PE in HCT116 cells. It has been reported that several dietary phytochemicals with proven chemopreventive and cell growth inhibition activities, modulate AP-1 transcription activation in colon cancer cells in vitro (Jeong, Kim, Hu, & Kong, 2004). AP-1 activity is involved in many diverse cellular processes including apoptosis, proliferation and transformation (Toh, Siddique, Boominathan, Lin, & Sabapathy, 2004). It was also found, as one of the most affected genes, the down-regulation of phosphodiesterase 4B (PDE4B), recognized as an apoptosis negative regulator (Smith et al., 2005); and also the aforementioned up-regulation of OSGIN1 is worth to mention. In overall, the regulation of this set of genes resulted in the prediction of downstream cell death increase as determined by IPA.

RKO highest scored canonical pathway was glutathione redox reactions 1. It is widely known that the downregulation of antioxidant enzymes, such as GPX8, GPX1 and GSR, can entail an increase of ROS inside the cells. Several studies have pointed out that imbalance between ROS production and antioxidant defenses lead to the disruption of cellular metabolism due to the chemical damage of proteins, lipids, polysaccharides and DNA. The degree of cellular damage determines the type of death mechanisms that are activated (Finkel & Holbrook, 2000). Similar to HCT116 cell line, some antioxidant response-related genes were upregulated in RKO, such as HMOX1 and GST.

Furthermore, the differential expression of genes caused by the treatment of AH-PE and BM-PE in RKO cell line, resulted in a significant predicted reduction of proliferation of tumor cells and G1/S phase transition as determined by IPA. RKO cells differential expression of genes highlight the down-regulation of melanoma-associated antigen 2 (MAGE-2) known to be present in CRC cells functioning as a cell viability promoter through binding to histone deacetylase and repressing p53-dependent apoptosis (Peche, Scolz, Ladelfa, Monte, & Schneider, 2012). Also a moderately up-regulation of growth arrest and DNA-damage-inducible protein alpha (GADD45A) and cyclin-dependent kinase inhibitor 1-A (CDKN1A), also known as p21, both encoded proteins are recognized as cell cycle inhibitors (Jin et al., 2000). In addition, RKO did not show significant modification of canonical pathways related to apoptosis or cell death, suggesting coexistence of cytostatic and cytotoxic effects induced by treatments with AH-PE and BM-PE.

It is worth noting the remarkable down-regulation of cytokeratin 19 (KRT19) in RKO, which has been found greatly expressed in highly metastatic CRC cells compared to poorly metastatic cells (Luque-García et al., 2010), and also expressed in metastatic tumors and circulating cancer cells in liver and breast (Ding et al., 2004; Sieuwerts et al., 2011). Cytokeratin 19 is a protein transcriptionally activated by hypoxia-induced factor 1 (HIF-1), which functions include the transcription of genes that are involved in crucial aspects of cancer biology, including angiogenesis, cell survival, glucose metabolism and invasion (Semenza, 2003). The role of cytokeratin 19 in metastasis and invasion is not completely understood, but it has been recognized to be related to cytoskeleton organization and cell adhesion, thus contributing with aggressiveness of cancer cells (De Angelis, Svendsrud, Kravik, & Stokke, 2006).

Our validation showed that RT-PCR results are in good agreement with microarray results for genes validated in HCT116 cell lines for both AH-PE and BM-PE extracts, with significant results in RT-PCR for PDE4B and OSGIN1 genes. These genes are highly associated with carcinogenesis. For instance, a recent study showed that PDE4B was highly expressed in clinical tumor samples from CRC patients. It is upregulated by oncogenic KRAS, its inhibition led to epithelial cell polarity and apoptosis in CRC and increased mRNA expression was associated with relapsed CRC in genome wide analysis of public data set (Tsunoda et al., 2012). Both microarray and RT-PCR results showed that PDE4B was downregulated by AH-PE and BM-PE treatments indicating the potential of these peptide extracts to reduce the activity of PDE4B which can lead to better management of CRC by increasing apoptosis and maintaining the epithelial characteristic of the cells which is important in preventing metastasis. On the other hand, validation of genes in RKO by RT-PCR showed that only AH-PE treatment agreed with microarray results specifically for KRT19 and EEF1A2 genes. Recent studies have shown that KRT19 is expressed in CRC patients with circulating tumor cells (de Albuquerque et al., 2012) while EEF1A2 decreased expression by p16 led to inhibition of cancer cell growth (Lee et al., 2013). Down-regulation of these genes then will have a positive impact in preventing the outgrowth of cancer cells which could possibly attained by AH-PE treatment.

RT-qPCR is a commonly used validation tool for microarray analysis. However, there are certain factors that might contribute when the correlations between these two techniques are analyzed. For instance, the lower correlation between microarray and qPCR for down-regulated genes may alternatively be due to the effects of greater variability associated with decreased reaction efficiencies found in qPCR measurements at later cycles, where genes with low expression levels respond (Morey, Ryan, & Van Dolah, 2006).

In conclusion, our results revealed for the first time that the common bean NDF peptides extracted from cultivars Azufrado Higuera and Bayo Madero affected gene expression profile of human colon cancer cells in vitro. The global response of HCT116 and RKO was the up-regulation of transcriptionally activated genes that encode antioxidant enzymes related to NRF-2. Although NRF-2-regulated high expression of antioxidant enzymes during chemotherapy, it has been reported to be cause of ineffectiveness of chemotherapeutic agents. Studies using NRF-2 knock-out cancer models have clearly shown the protective role of NRF-2 in cancer prevention particularly during the earlier phases of initiation of carcinogenesis (Hu, Saw, Yu, & Kong, 2010). Thus, for HCT116 cell line, AH-PE and BM-PE treatments can lead to the induction of apoptosis and cell death. For RKO cell line, AH-PE and BM-PE have both cytostatic and cytotoxic effects related to ROS imbalance. In addition to these pathways affected by peptide extract treatments, we also found genes that were downregulated including PDE4B and KRT19 that have potential role in cancer proliferation and apoptosis. The microarray-based prediction presented in this study allowed investigating interesting signaling pathways to elucidate the effect of peptide extract from the NDF of common bean in human CRC in vitro. This study found 8 DEGs to be similar for both cell lines triggered by both bean cultivars, namely C11orf31, C9orf169, EMP1, GEM, PLIN2, SUN3, TRIM16L and TXNRD1. For the first time, the present study discovered genes modulated in vitro in HCT116 and RKO human colon cancer cells due to the treatment with peptide extracts from common beans.

There are several factors to consider in future studies; for instance, to elucidate a concrete mechanism of action evaluating pure bean peptides in in vitro and in vivo models of CRC.

Acknowledgements

Author Diego A. Luna Vital was supported by a scholarship from the Consejo Nacional de Ciencia y Tecnologia CONACyT—Mexico. This research was supported by a Universidad Autónoma de Querétaro—University of Illinois Small Research Grants Program UAQ MOU/OIP Match.

Appendix A. Supplementary data

Supplementary data to this article can be found online at http://dx.doi.org/10.1016/j.foodres.2014.02.037.

References

American Type Culture Collection (2013). Available from. http://www.atcc.org (Accessed on October 29th)

Aparicio-Fernandez, X., Manzo-Bonilla, L., & Loarca-Piña, G. (2005). Comparison of antimutagenic activity of phenolic compounds in newly harvested and stored common beans (*Phaseolus vulgaris*) against Aflatoxin B_1. *Journal of Food Science*, *70*, S73–S78.

Awwad, R. A., Sergina, N., Yang, H., Ziober, B., Willson, J. K. V., Zborowska, E., et al. (2003). The role of transforming growth factor alpha in determining growth factor independence. *Cancer Research*, *63*, 4731–4738.

Benjamini, Y., & Hochberg, Y. (1995). Controlling the false discovery rate: A practical and powerful approach to multiple testing. *Journal of the Royal Statistical Society B*, *57*, 289–300.

Buthia, S. K., & Maiti, T. K. (2008). Targeting tumors with peptides from natural sources. *Cell*, *4*, 210–217.

Campos-Vega, R., García-Gasca, T., Guevara-González, R., Ramos-Gómez, M., Oomah, B.D., & Loarca-Piña, G. (2012). Human gut flora-fermented nondigestible fraction from cooked bean (*Phaseolus vulgaris* L.) modifies protein expression associated with apoptosis, cell cycle arrest, and proliferation in human adenocarcinoma colon cancer cells. *Journal of Agricultural and Food Chemistry*, *60*, 12443–12450.

de Albuquerque, A., Kubisch, I., Stolzel, U., Ernst, D., Boese-Landgraf, J., Breier, G., et al. (2012). Prognostic and predictive value of circulating tumor cell analysis in colorectal cancer patients. *Journal of Translational Medicine*, *10*, 222.

De Angelis, P.M., Svendsrud, D. H., Kravik, K. L., & Stokke, T. (2006). Cellular response to 5-fluorouracil (5-FU) in 5-FU-resistant colon cancer cell lines during treatment and recovery. *Molecular Cancer*, *5*, 20.

Dia, V. P., & de Mejía, E. G. (2010). Lunasin promotes apoptosis in human colon cancer cells by mitochondrial pathway activation and induction of nuclear clusterin expression. *Cancer Letters*, *295*, 44–53.

Dia, V. P., & de Mejía, E. G. (2011). Lunasin induces apoptosis and modifies expression of genes associated with extracellular matrix and cell adhesion in human metastatic colon cancer cells. *Molecular Nutrition and Food Research*, *55*, 623–634.

Ding, S. J., Li, Y., Tan, Y. X., Jiang, M. R., Tian, B., Liu, Y. K., et al. (2004). From proteomic analysis to clinical significance: Overexpression of cytokeratin 19 correlates with hepatocellular carcinoma metastasis. *Molecular and Cellular Proteomics*, *3*, 73–81.

Ferlay, J., Shin, H. R., Bray, F., Forman, D., Mathers, C., & Parkin, D.M. (2013). GLOBOCAN 2008 v2.0, Cancer incidence and mortality worldwide: IARC CancerBase No. 10. Lyon, France. Available from: http://globocan.iarc.fr (accessed on November 1st)

Finkel, T., & Holbrook, N. J. (2000). Oxidants oxidative stress and the biology of ageing. *Nature*, *408*, 239–247.

Gentleman, R., Carey, V. J., Bates, D.M., Bolstad, B., Dettling, M., Dudoit, S., et al. (2004). Bioconductor: Open software development for computational biology and bioinformatics. *Genome Biology*, *5*, R80.

González de Mejía, E., Wang, W., & Dia, V. P. (2010). Lunasin with an arginine–glycine–aspartic acid motif causes apoptosis to L1210 leukemia cells by activation of caspase-3. *Molecular Nutrition and Food Research*, *54*, 406–414.

Hsieh, C. C., Hernandez-Ledesma, B., & de Lumen, B. O. (2011). Cell proliferation inhibitory and apoptosis-inducing properties of anacardic acid and lunasin in human breast cancer MDA-MB-231 cells. *Food Chemistry*, *125*, 630–636.

Hsieh, C. C., Hernandez-Ledesma, B., Jeong, H. J., Park, J. H., & de Lumen, B. O. (2010). Complementary roles in cancer prevention: protease inhibitor makes the cancer preventive peptide lunasin bioavailable. *PLos One*, *5* (Art. e8890).

Hu, R., Saw, C. L. L., Yu, R., & Kong, A. N. T. (2010). Regulation of NF-E2-related factor 2 signaling for cancer chemoprevention: Antioxidant coupled with anti-inflammatory. *Antioxidant and Redox Signaling*, *13*, 1679–1698.

Huang, D. W., Sherman, B. T., & Lempicki, R. A. (2009). Bioinformatics enrichment tools: Paths toward the comprehensive functional analysis of large gene lists. *Nucleic Acids Research*, *37*, 1–13.

Huang, D. W., Sherman, B. T., & Lempicki, R. A. (2009). Systematic and integrative analysis of large gene lists using DAVID bioinformatics resources. *Nature Protocols*, *4*, 44–57.

Jeong, W. S., Kim, I. W., Hu, R., & Kong, A. N. T. (2004). Modulation of AP-1 by natural chemopreventive compounds in human colon HT-29 cancer cell line. *Pharmaceutical Research*, *21*, 649–660.

Jin, S., Antinore, J., Lung, F. T., Dong, X., Zhao, H., Fan, F., et al. (2000). The GADD45 inhibition of cdc2 kinase correlates with GADD45-mediated growth suppression. *Journal of Biological Chemistry*, *275*, 16602–16608.

Joyce, T., Cantarella, D., Isella, C., Medico, E., & Pintzas, A. (2009). A molecular signature for epithelial to mesenchymal transition in a human colon cancer cell system is revealed by large-scale microarray analysis. *Clinical & Experimental Metastasis*, *26*, 569–587.

Lanza, E., Hartman, T. J., Albert, P.S., Shields, R., Slattery, M., Caan, B., et al. (2006). High dry bean intake and reduced risk of advanced colorectal adenoma recurrence among participants in the polyp prevention trial. *Journal of Nutrition*, *136*, 1896–1903.

Lee, M. H., Choi, B. Y., Cho, Y. Y., Lee, S. Y., Huang, Z., Kundu, J. K., et al. (2013). Tumor suppressor p16 (INK4a) inhibits cancer cell growth by downregulating EEF1A2 through a direct interaction. *Journal of Cell Science*, *126*, 1744–1752.

Lee, J. S., & Surh, Y. J. (2005). Nrf2 as a novel molecular target for chemoprevention. *Cancer Letters*, *224*, 171–184.

Luque-García, J. L., Martínez-Torrecuadrada, J. L., Epifano, C., Cañamero, M., Babel, I., & Casal, J. I. (2010). Differential protein expression on the cell surface of colorectal cancer cells associated to tumor metastasis. *Proteomics*, *10*, 940–952.

Matsubara, J., Honda, K., Ono, M., Sekine, S., Tanaka, Y., Kobayashi, M., et al. (2011). Identification of adipophilin as a potential plasma biomarker for colorectal cancer using label-free quantitative mass spectrometry and protein microarray. *Cancer Epidemiology, Biomarkers and Prevention*, *20*, 2195–2203.

Megías, C., Yust, M., Pedroche, J., Lquari, H., Giron-Calle, J., & Alaiz, M. (2009). Purification of an ACE inhibitory peptide after hydrolysis of sunflower (*Helianthus annuus* L.) protein isolates. *Journal of Agricultural and Food Chemistry*, *52*, 1928–1932.

Méplan, C., & Hesketh, J. (2011). The influence of selenium and selenoprotein gene variants on colorectal cancer risk. *Mutagenesis*, *27*, 177–186.

Morey, J. S., Ryan, J. C., & Van Dolah, F. M. (2006). Microarray validation: Factors influencing correlation between oligonucleotide microarrays and real-time PCR. *Biological Procedures Online*, *8*, 175–193.

Peche, L. Y., Scolz, M., Ladelfa, M. F., Monte, M., & Schneider, C. (2012). MageA2 restrains cellular senescence by targeting the function of PMLIV/p53 axis at the PML-NBs. *Cell Death and Differentiation*, *19*, 926–936.

Pedroche, J., Yust, M., Girón-Calle, J., Alaiz, M., Millán, F., & Vioque, J. (2002). Utilisation of chickpea protein isolates for production of peptides with angiotensin I-converting enzyme (ACE)-inhibitory activity. *Journal of the Science of Food and Agriculture*, *82*, 960–965.

Pirooznia, M., Nagarajan, V., & Deng, Y. (2007). GeneVenn—A web application for comparing gene lists using Venn diagrams. *Bioinformation*, *1*, 420–422.

R Development Core Team (2013). *R: A language and environment for statistical computing.* Vienna, Austria: R Foundation for Statistical Computing3-900051-07-0 (URL http://www.R-project.org/).

Ritchie, M. E., Diyagama, D., Neilson van Laar, R. J., Dobrovic, A., Holloway, A., & Smyth, G. K. (2006). Empirical array quality weights in the analysis of microarray data. *BMC Bioinformatics*, *7*, 261–277.

Saura-Calixto, F., García-Alonso, A., Goñí, I., & Bravo, L. (2000). In vitro determination of the indigestible fraction in foods: An alternative to dietary fiber analysis. *Journal of Agricultural and Food Chemistry*, *48*, 3342–3347.

Semenza, G. (2003). Targeting HIF-1 for cancer therapy. *Nature Reviews Cancer*, *3*, 721–732.

Sieuwerts, A., Mostert, B., Bolt-de Vries, J., Peeters, D., de Jongh, F. E., Stouthard, J. M. L., et al. (2011). mRNA and microRNA expression profiles in circulating tumor cells and primary tumors of metastatic breast cancer patients. *Clinical Cancer Research*, *17*, 3600–3618.

Slattery, M., Lundgreen, A., Welbourn, B., Corcoran, C., & Wolff, R. (2012). Genetic variation in selenoprotein genes, lifestyle, and risk of colon and rectal cancer. *PLos One*, *7*, e37312.

Smith, P. G., Wang, F., Wilkinson, K. N., Savage, K. J., Klein, U., Neuberg, D. S., et al. (2005). The phosphodiesterase PDE4B limits cAMP-associated Pi3K/AKT-dependent apoptosis in diffuse large B-cell lymphoma. *Blood*, *105*, 308–316.

Smyth, G. K. (2004). Linear models and empirical Bayes methods for assessing differential expression in microarray experiments. *Statistical Applications in Genetics and Molecular Biology*, *3* (Article 3).

Smyth, G. K. (2009). Limma: Linear models for microarray data. In R. Gentleman, V. Carey, S. Dudoit, R. Irizarry, & W. Huber (Eds.), *Bioinformatics and Computational Biology Solutions using R and Bioconductor*. : Springer.

Smyth, G. K., Michaud, J., & Scott, H. (2005). The use of within-array replicate spots for assessing differential expression in microarray experiments. *Bioinformatics*, *21*, 2067–2075.

Smyth, G. K., & Speed, T. P. (2003). Normalization of cDNA microarray data. *Methods*, *31*, 265–273.

Toh, W. H., Siddique, M. M., Boominathan, L., Lin, K. W., & Sabapathy, K. (2004). c-Jun regulates the stability and activity of the p53 homologue, p73. *Journal of Biological Chemistry*, *279*, 44713–44722.

Tsunoda, T., Ota, T., Fujimoto, T., Doi, K., Tanaka, Y., Yoshida, Y., et al. (2012). Inhibition of phosphodiesterase-4 (PDE4) activity triggers luminal apoptosis and AKT dephosphorylation in a 3-D colonic crypt model. *Molecular Cancer*, *11*, 46.

Valdés, A., García-Cañas, V., Rocamora-Reverte, L., Gómez-Martínez, A., Ferragut, J. A., & Cifuentes, A. (2013). Effect of rosemary polyphenols on human colon cancer cells: Transcriptomic profiling and functional enrichment analysis. *Genes and Nutrition*, *8*, 43–60.

Vergara-Castañeda, H. A., Guevara-González, R. G., Guevara-Olvera, B.L., Oomah, B.D., & Loarca-Piña, G. F. (2012). Non-digestible fraction of beans (*Phaseolus vulgaris* L.) modulates signaling pathway genes at an early stage of colon cancer in Sprague–Dawley rats. *British Journal of Nutrition*, *108*, S145–S154.

Vergara-Castañeda, H. A., Guevara-González, R. G., Ramos-Gómez, M., Reynoso-Camacho, R., Guzmán-Maldonado, H., Feregrino-Pérez, A. A., et al. (2010). Non-digestible fraction of cooked bean (*Phaseolus vulgaris* L.) cultivar Bayo Madero suppresses colonic aberrant crypt foci in azoxymethane-induced rats. *Food and Functions*, *1*, 294–300.

Wang, T., Xia, D., Li, N., Wang, C., Chen, T., Wan, T., et al. (2005). Bone marrow stromal cell-derived growth inhibitor inhibits growth and migration of breast cancer cells via induction of cell cycle arrest and apoptosis. *Journal of Biological Chemistry*, *280*, 4374–4382.

Wolin, K. Y., Carson, K., & Colditz, G. A. (2010). Obesity and cancer. *The Oncologist*, *15*, 556–565.

Yao, H., Li, P., Venters, B. J., Zheng, S., Thompson, P. R., Pugh, F., et al. (2006). Histone Arg modifications and p53 regulate the expression of OKL38, a mediator of apoptosis. *Journal of Biological Chemistry*, *283*, 20060–20068.